Research and Optimization of Charging Pile Demand Forecasting Model Based on Data Mining

Tao Jin^{1*}, Bin Liu, Zhenqi Zhang School of Information Eegineering, Yinchuan University of Science and Technology *Corresponding author: chong214@163.com

Keywords: electric vehicle (EV), charging pile demand forecasting, infrastructure optimization, energy management, mandrill-tuned convolutional long short memory with auto encoder (MCLSM-AE)

Recieved: May 9, 2025

The rapid growth of electric vehicles (EVs) has led to a significant increase in the demand for accurate forecasting of charging pile usage, essential for optimizing infrastructure planning and energy management. Effective prediction models help to balance grid loads, reduce waiting times, and enhance the overall charging experience. Existing methods, based on traditional Machine Learning (ML) or basic neural network models, struggle to capture complex spatial-temporal relationships and multivariate dependencies. To address these limitations, this research proposes an advanced hybrid Mandrill-tuned Convolutional Long Short Memory with Auto Encoder (MCLSM-AE) framework that combines the Mandrill Optimization Algorithm (MOA), Auto Encoder (AE), and CNN-LSTM with an Attention Mechanism. The novelty of this approach lies in integrating MOA for optimal hyper parameter tuning, AE for dimensionality reduction and CNN-LSTM for spatial-temporal demand modeling, enhanced with an attention mechanism for improved interpretability. The model is trained on a dataset comprising historical EV charging data, traffic patterns, weather information, and spatial grid mappings. Preprocessing steps include data normalization and Missing Value Imputation (MVI) to ensure data quality. The proposed model workflow involves reducing data dimensionality with AE, extracting spatial patterns with CNN, and capturing temporal dependencies using LSTM, with MOA optimizing model parameters. Experimental results demonstrate the suggested MCLSM-AE model superior performance, achieving a MSE (0.00000000022) RMSE of (0.000014832), and MAE (0.0275) compared to existing methods. The research provides a robust and scalable solution for EV charging demand forecasting, addressing existing limitations and contributing to better infrastructure and energy management strategies

Povzetek: Študija je razvila hibridni model MCLSM-AE, ki združuje mandrillovo optimizacijo, AutoEncoder, CNN-LSTM in pozornost za napovedovanje povpraševanja po polnilnicah električnih vozil. Model učinkovito obdela prostorsko-časovne podatke ter doseže izjemno nizke napake, kar podpira optimalno energetsko in infrastrukturno načrtovanje.

1 Introduction

The Electric Vehicle (EV) sector has developed as the most important socially sustainable technology, with enormous potential for reducing carbon dioxide emissions while lowering dependency on oil [1]. EVs are a crucial solution for reducing the transportation sector's massive greenhouse gas emissions. The fast development of EVs is partly dependent on the building and arrangement of charging facilities [2]. The great amount of EVs associated with the grid creates an enormous strain on the electrical grid [3]. The rapid popularization of new Electric Vehicles (EVs),

primarily its extensive promotion in various countries, relies heavily on the presence of charging facilities, like Charging Piles (CP), CP are a critical element in the period of electrified transportation, providing important fast charging service stations for new EVs, ensuring that daily travel demands are fulfilled and promoting the widespread adoption of EVs [4]. There are two categories of CPs such as DC quick charging and Alternating Current (AC) slow charging. The service style is self-pay and self-charge, and the locations are much more spread out than petrol stations [5]. Charging infrastructure has a huge impact on the growth of EVs due to its accessibility, dependability,

cost efficiency, smart networking, and environmental sociability [6]. However, inadequate charging services have developed as a key impediment for the EV sector. As EVs become more prevalent in urban areas, it is becoming more difficult to predict Charging Demand (CD) and plan for infrastructure [7]. To overcome the above challenges, the research proposed an advanced hybrid Mandrill-tuned Convolutional Long Short Memory with Auto Encoder (MCLSM-AE) framework that combines the Mandrill Optimization Algorithm (MOA), AutoEncoder (AE), and CNN-LSTM with an Attention Mechanism to develop a robust and scalable forecasting model for EVCP demand. This research offers a strong framework on EV charging demand prediction that may be utilized for better infrastructure development, grid load balancing, and user experience. For data-oriented policy and planning related to the

long-term adoption of electric vehicle networks, it is especially beneficial for policy makers, utility companies, urban planners, and charging station operators.

The organization of the research contains the following sub divisions. Section 2 contains the related work and Section 3 explains the methods used to forecast the Electric VehicleCharging Demand (EVCD). The outcomes of the method were performed and discussed in Section 4. The research concluded in Section 5.

2 Related work

The research was compared with existing research as shown in the Table 1, which represents the summary of literature on EV charging demand forecasting.

Table 1: Summary of literature on EV charging demand forecasting

Ref. No.	Area Focused	Algorithms/Models Used	Result	Limitations
[8]	Urban EV quick charging demand forecasting	Regret Theory, Human behavior modeling, Data mining	Improved CD forecast accuracy using real ridehailing data	Limited scalability due to localized data from Nanjing
[9]	EV public charging demand forecasting	Demand-supply stochasticity model, User heterogeneity modeling	High-resolution spatial-temporal forecasts	Assumptions in user behavior; uncertainty in future transport networks
[10]	EVCD forecasting under noisy data	CFMM-GEP (AutoEncoder + SVM + GEP)	Outperformed 6 models in MAPE, RMSE, MAE, R ²	Impacted by complex or irregular noise patterns
[11]	Charging station (CS) planning with multi-type CDs	Firefly algorithm, Roulette, K-Means, Markov Chain	Reduced cost and improved efficiency in real urban setting	Assumptions in user travel behavior; data uncertainty
[12]	Smart charging and private charging piles	Simulation-based modeling	Shifted peak load, improved charging profile	Based on one city's data; lacks generalizability
[13]	Automated charging infrastructure	1-to-N system, robotic arm, 2-layer iterative scheduling	Validated in real- time via hardware- in-loop experiments	High implementation cost; scalability issues
[14]	EV charging infrastructure deployment	Submodular functions, Erlang-loss, Lazy Greedy (LGDG & LGEG)	High efficacy and efficiency in site planning	May struggle in highly dynamic and complex environments
[15]	Smart EV-CP management system	IoT, K-Means, Multisim simulation	Reduced cost, improved voltage stability and user experience	Simulation-based validation only; needs real-world testing
[16]	Spatial-temporal distribution of EV load	Monte Carlo simulation	Showed distinct regional and	Requires detailed regional data; may not generalize globally

			temperature-based load variation	
[17]	EV charging prediction using UrbanEV dataset	DL models, Transformer, statistical models	Improved forecast accuracy	Regional focus (Shenzhen); potential bias due to geography/weather
[18]	Citywide EVCD prediction	CityEVCP (Hypergraph + POI clustering + Gated Transformer)	Outperformed baseline models in spatial-temporal accuracy	Scalability challenges in larger cities; POI data dependence
[19]	EV-CS position and capacity optimization	NSGA-II, Deep Learning, Queueing Theory	Enhanced efficiency, reduced waiting time	Difficulty estimating computational complexity; uncertain service rates
[20]	Short-term EVCD forecasting with private EVs	LSTM, compared with ARIMA, MLP	LSTM outperformed others (MAPE = 6.83%)	Prediction depends heavily on data interval and input structure
[21]	Short/long-term EVCD forecasting	Transformer, RNN, LSTM, ARIMA, SARIMA	Transformer achieved highest accuracy	Requires large data volumes for generalization and robustness

The existing model [8] was not scalable since it used Nanjing-specific data, and hence it would not be effective for other regions or large datasets. CFMM-GEP [10] contained complex or unusual noise patterns that influence the model's performance. The [14] method utilized submodular functions and Lazy Greedy algorithms to struggle with dynamic and complex environments; it might not be ideal for infrastructure deployment under dynamic conditions. Lastly, the method outlined in [19] that combined NSGA-II, deep learning, and queueing theory was facing the challenge of forecasting computing complexity and dealing with uncertain service rates, which can limit its performance in real-time optimization. To address these limitations, the research proposed an advanced hybrid MCLSM-AE framework.

Materials and methods

The research aimed to develop a robust and accurate forecasting model for the EVCD using the proposed advanced hybrid MCLSM-AE model. The model is trained on a dataset comprising historical EV charging data, traffic patterns, weather information, and spatial grid mappings. Data preprocessing includes data normalization and MVI to verify data quality. The MCLSM-AE method was used for predicting EVCD. The MCLSM-AE method design for prediction of EVCD is shown in Figure 1.

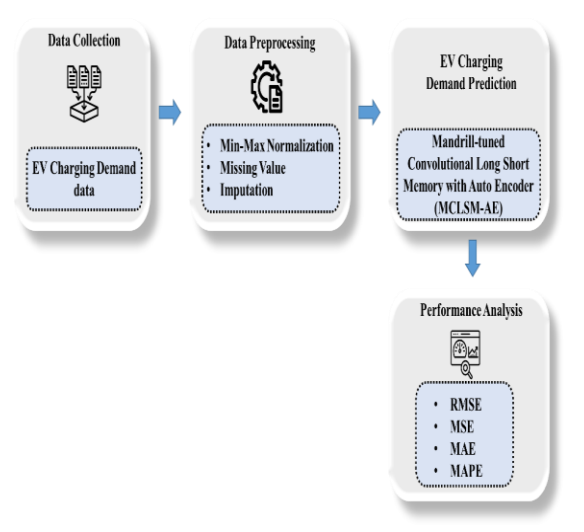


Figure 1: Structure for proposed framework to predict the electric vehiclescharging demand

3.1 Data collection

The data was gathered from Kaggle Link: https://www.kaggle.com/datasets/ziya07/chargingpile-demand-forecasting-dataset/data. The Charging Demand Dataset Pile Forecasting offers comprehensive information for forecasting how often electric vehicle (EV) charging piles will be used. This dataset contains a number of characteristics that affect the need for charging, including charging time, energy usage, traffic patterns, meteorological conditions, and geographic considerations. In order to accurately simulate real-world situations, it also takes into account variables like car type, charging station density, and

government incentives. The percentage of time spent using a charging pile is represented by the goal variable, charging_pile_usage_rate, which is essential for improving energy management and infrastructure planning in the expanding electric car market. By reducing wait times, balancing grid loads, and enhancing user experience, this dataset seeks to support the development of predictive models for effective EV charging stations. Table 2 show the overall dataset features. The data was split into testing and training with 80:20 ratio.

Table 2: Overall dataset features

Feature	Description
Charging Duration	Duration for which EVs use
	the charging pile (in hours).
Energy Consumed	Total energy consumed
	during charging (in kWh).
Traffic Flow	Number of vehicles passing
	through the charging
	station area.
Weather Conditions	Includes temperature,
	humidity, precipitation,
	and wind speed.
Geographical	Location-based features
Information	such as latitude, longitude,
	and distance to the nearest
	road.
Charging Price and	Charging price per kWh
Incentives	and availability of
	government incentives.

3.2 Data preprocessing

Data preprocessing is a process of converting raw data into an organized form that can improve the performance of the ML models. It facilitates the handling of inconsistency, noise, and missing values, resulting in consistent inputs for training. EV charging data were preprocessed by normalization using Min-Max Normalization and imputation using Multiple Imputation (MI). The Min-Max Normalization was applied to normalize EVCD data to the same range. MI was used to impute missing values that ensured completeness of data.

3.2.1 Data normalization

Data Normalization is used for normalizing numerical data into the standard range, typically between 0 and 1, thus allowing the different features of different magnitudes and different units not to dominate the process of model learning. Min-Max Normalization has been used in the normalization of the EV charging data. Min-Max Normalization is also employed to map historic EVCD data, traffic flow patterns, weather states, and grid space values onto the same scale. This approach applies the following Eq. (1).

$$Y_{new} = \frac{Y - min(Y)}{max(Y) - min(Y)}$$
 (1)

Where Y is the old value, max(Y) is the dataset's maximum value, min(Y) is its minimum value, and Y_{new} is the new value derived from the normalized findings.

3.2.2 Missing value imputation (MVI)

MVI refers to the process of filling missing or incomplete data points with imputed values to maintain the integrity of the dataset. It ensures accurate EVCD forecasting by maintaining spatial-temporal data integrity despite missing records. MVI was applied using MI to deal with missing data-induced uncertainty and bias when EVCD is forecasted. The final parameter estimates, $\bar{\beta}$ are produced by pooling these values as given in Eq. (2).

$$\bar{\beta} = \frac{1}{n} \sum_{m=1}^{n} \hat{\beta}_m \tag{2}$$

Where $\bar{\beta}$ represents the final pooled parameter estimate, n is the number of imputed datasets, and $\hat{\beta}_m$ refers to the parameter estimates from each m^{th} imputed dataset.

3.3 Charging pile demand forecasting model using mandrill-tuned convolutional long short memory with auto encoder (MCLSM-AE)

MCLSM-AE integrates MOA's hyperparametertuning, uses CNNto extract spatial features, enabling such that the model can identify complex patterns in the data, and LSTM networks are utilized for extracting temporal dependencies, which are important in precisely predicting future EV charging demands. AE dimensionally compresses the data, which simplifies the data and makes the model more efficient by preserving only important features. This methodology maximizes the model's capability to estimate complex, multivariate, and spatial temporal demand patterns of EV CS. MOA was incorporated into MCLSM-AE to improve model performance by tuning parameters while AE's dimensionality reduction helpssimplify complex data and retain essential features. The combination helps make prediction performance reasonable in real-world scenarios, where functions have complex, non-linear relationships, and multiple influencing factors.

3.3.1 AutoEncoder (AE)

An AE is an unsupervised neural network that compresses input into lower-dimensional representations before reconstructing it to determine the quality of retrieved features. It is used to extract critical spatial-temporal elements from upstream and downstream EVCD data, hence improving forecasting accuracy. A function f is used to obtain the characteristic sequence of an original input sequence

 $Y = \{y_1, y_1, \dots, y_k\}$, where $y_i \in \mathbb{R}^d$. The output T = $\{t_1, t_2, \dots, t_k\}$, where $t_i \in \mathbb{R}^l$, reflects the encoded properties of X. The encoder's output is provided to the decoder, which reconstructs the original data from T, resulting in $Z = \{z_1, z_1, \dots, z_k\}$, where $z_i \in \mathbb{R}^d$. After training the AE, the encoder is used for feature extraction, revealing the data's underlying structure. Eq. (13) and (14) determines the encoding and decoding operation.

$$t_j = f(w_t \cdot y_j + c_t) \tag{13}$$

$$z_j = g(w_z \cdot t_j + c_z) \tag{14}$$

Where w_t , w_z , c_t , and c_z are weights and biases, respectively, and $f(\cdot)$ and $g(\cdot)$ are sigmoid functions. $y_i \in \mathbb{R}^d$ is the original input vector of dimension d, the encoder weight matrix is given by w_t , and c_t is the encoder bias. $t_i \in \mathbb{R}^l$ is the encoded feature from the encoder, the decoder weight matrix is w_z , and c_z is the decoder bias. Eq. (15) states that the AE is trained by minimalizing the reconstruction error.

$$L(Y,Z) = \frac{1}{2} \sum_{j=1}^{n} ||y_j - z_j||^2$$
 (15)

This is a loss function calculates the rebuilding error between the input (y_i) and output (z_i) . The Mean Squared Error (MSE) is calculated by over all n samples to ensure the encoder captures significant data characteristics. When the reconstruction error is sufficiently small, T is considered a valid representation of the original data. Let $Y_v =$ $\{y_{v1}, y_{v2}, \dots, y_{vm}\}$ and $Yd = \{yd_1, yd_2, \dots, yd_m\},$ where y_{vj} , $yd_j \in \mathbb{R}^d$, be the upstream and downstream charging load data. The characteristic sequence x_t = $\{x_1, x_2, \dots, x_m\}$, with $x_i \in \mathbb{R}^l$, is calculated using Eq.(16) and (17).

$$x_j = f(w_z \cdot (y_{vj} + y_{ej}) + c_x)$$
 (16)

$$z_j = g(w_z \cdot x_j + c_z) \tag{17}$$

 $y_{vj} \in \mathbb{R}^d$ are the upstream and downstream traffic flow vectors, w_z is the encoder weight and c_x is the bias. x_i is the encoded feature of combined traffic flow, w_z and c_z are decoder weights and bias. $g(\cdot)$ is the sigmoid function producing the reconstructed output z_i , helping assess the effectiveness of the encoded features.

3.3.2 Convolutional long short memory with auto encoder (CLSM-AE)

The CLSM-AE combines CNN with LSTM and AE: CNN can be used to extract the specialcharacteristics, LSTM can be used to extract the temporal dynamics and AE can be used to boil down the dataset into lower dimensions. The capacity to extract both temporal and spatial characterizations with dimensional reduction offers a sound and powerful forecasting method for complex and high-dimensional patterns of EVCD in spatial-temporal situations.

Convolutional long 3.3.3. short memory withattention mechanism

The model has two LSTM layers, an attention layer, single input layer, two convolution layers, and a single output layer. The input is first given to the model and the local characteristics are retrieved using CNN layers. The CNN layer's outputs are passed to the first LSTM layer to extract long-range relationships among variables. The attention layer leverages the hidden states of all LSTM layers to determine relevance for themselves. Finally, a weighted sum computes the output.

3.3.4. Convolutional neural networks (CNN)

CNN is a type of DL model that extracts spatial patterns and characteristics from data, such as images or grids. CNN is utilized to capture spatial dependencies in EVCD data, allowing for more accurate predictions by modeling the spatial distribution of CS and traffic patterns. The one-dimensional convolutional layer (Convld) receives the input $Y = \{y_1, y_2, \dots, y_T\}$, which is specified by Eq. (3).

$$g_l = ELU (W_m Y + b_m) (3)$$

Where g_l is m^{th} filter output, the activation function is represented by ELU, W_m is a matrix of weights and the bias vector is represented by b_m .

3.3.5. Long Short-Term Memory (LSTM)

LSTM is a type of Recurrent Neural Network (RNN) that predicts the long-term associations in sequential input. LSTM was utilized to describe the temporal dependencies in EVCD, allowing the forecasting model to consider historical charging patterns and more correctly estimate future demand over time. The outputs of the convolutional layers were given to the layer of the LTSM. There arethree gates, such as input, forget and output gate, and cell state. The forget gate removed some data in the first step and the input gate chooses which type of data is kept in the cell state, as shown in Figure 2. Eq. (4) to (6) provides the equations for these gates.

$$f_t = \sigma \left(W_f \cdot [g_{t-1}, \bar{y}_t] + b_f \right) \tag{4}$$

$$f_{t} = \sigma (W_{f} \cdot [g_{t-1}, \bar{y}_{t}] + b_{f})$$

$$i_{t} = \sigma (W_{i} \cdot [g_{t-1}, \bar{y}_{t}] + b_{i})$$

$$\tilde{C}_{t} = ELU (W_{C} \cdot [g_{t-1}, \bar{y}_{t}] + b_{C})$$
(6)

$$C_t = ELU\left(W_C \cdot [g_{t-1}, \bar{y}_t] + b_C\right) \tag{6}$$

Where g_{t-1} is represented as hidden state of t – 1, forget gate is given by f_t , W is the weight matrix of the respective gate, $\overline{\boldsymbol{y}}_t$ is the input of the layer in the time t, the bias of three gates is given by b,i_t is the input gate and C_t is the candidate value. The state of the cell at time t is depicted by the input gate i_t and C_t . Finally, the output gate (o_t) determines the current output as given by Eq. (7) to (9).

$$C_t = f_t * C_{t-1} + i_t * C_t \tag{7}$$

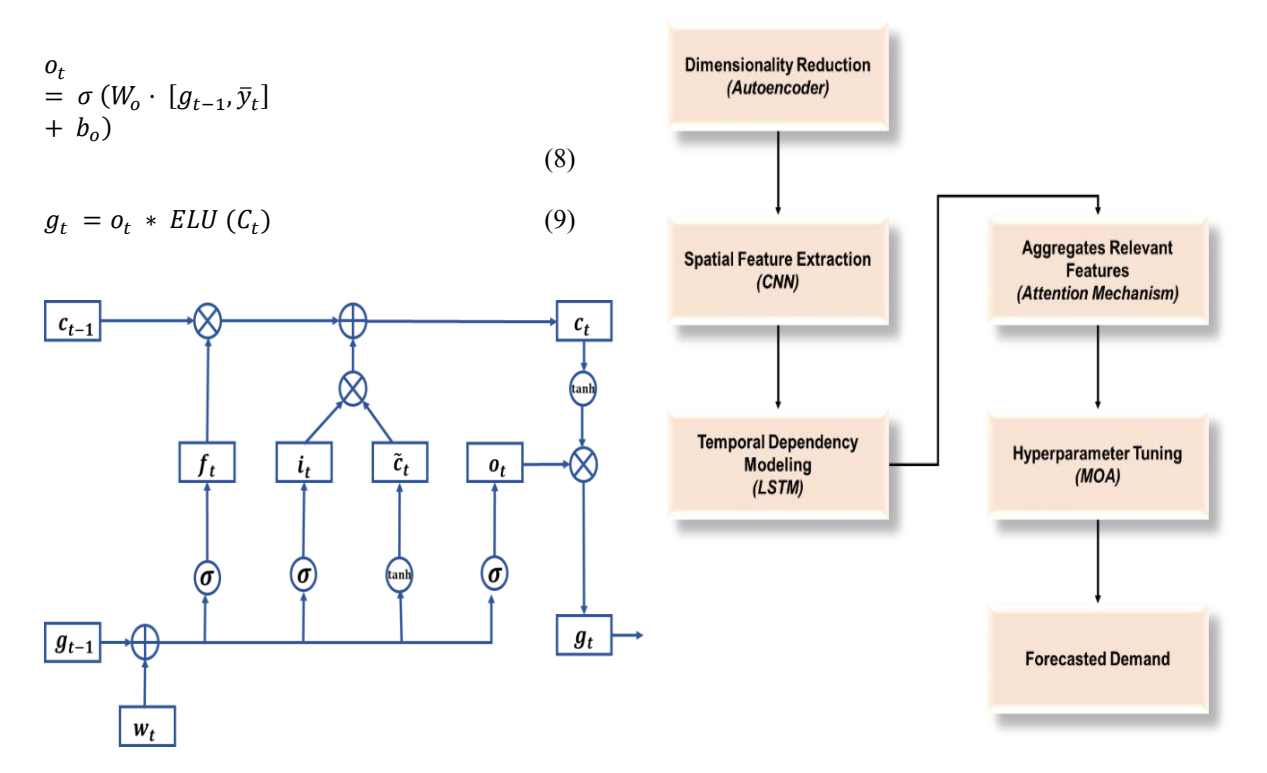


Figure 2: Architecture of LSTM

3.4 Attention mechanism

The Attention Mechanism is a DL approach that allows the model to focus on significant parts of the input data, weighting relevant characteristics and ignoring less important features. It was utilized to prioritize crucial spatial-temporal information in EVCD forecasting, resulting in improved accuracy and interpretability. After the LSTM layers have pulled out the long-term dependences from the features, it will take their output and use it as input for the attention layer. The necessary equations are as follows in Eq. (10) to (12).

$$a_{t}^{k} = \frac{\exp a_{t}^{k}}{\sum_{j=1}^{n} d_{t}^{j}}$$

$$d_{t}^{k} = v_{d}^{T} \sigma \left(W_{e} \left[g_{t-1}, c_{t-1} \right] + U_{d} g_{t} + c_{d} \right)$$

$$\bar{z}_{t} = \sum_{t}^{T} a_{t}^{T} g_{t}$$

$$(12)$$

The variables $v_e, c_d \in R^T$, $W_e \in R^{T \times m}$ and $U_d \in R^{m \times m}$ was learned, while m denotes the number of neurons, the output of the attention layer utilizing a weighted sum of all the hidden states is \bar{z}_t , and the attention weights of the k^{th} input at time t are denoted by a_t^k and d_t^k denote the significance of the g_t . The structure for the CLSM with Attention Mechanism was illustrated in Figure 3.

Figure 3: Structure of MCLSM-AE

3.5. Mandrill optimization (MO)

MO is a swarm intelligence-based metaheuristic inspired by mandrills' natural social structure and behavior. It is used to improve the spatial-temporal EVCD forecasting model by balancing exploration and exploitation for higher prediction accuracy. The particles are represented as a matrix with each row representing a particle's whole location as given by Eq. (18), where d is the amount of dimensions and n is the total amount of mandrills.

$$P = \begin{bmatrix} p_{1,1} & p_{1,2} & \dots & \dots & p_{1,d} \\ p_{2,1} & p_{2,2} & \dots & \dots & p_{2,1} \\ \vdots & \vdots & \dots & \dots & \vdots \\ p_{n,1} & p_{n,2} & \dots & \dots & p_{n,d} \end{bmatrix}$$
(18)

The technique of calculating and changing these places is described in mathematical terms. Initially, these places are produced semi-randomly and this process known as the initialization stage. Once each particle is allocated a place and, as a result, a fitness value, the positions are updated using the mathematical model of hierarchical dominance observed in mandrill hordes. The objective function F(x), optimized by the Mandrill Optimization Algorithm, is defined as the Mean Squared Error (MSE) computed on the validation set predictions during training.

3.6 Initialization phase

During this phase, research provides a semi-greedy initialization strategy. The first dimension of the search space is split into segments equal to the number of particles, guaranteeing that each particle is assigned to a unique segment along this dimension. For the remaining dimensions, particle placements are given at random, bringing variation to the starting population.

3.7 Dominator assignment

The next stage is to identify the dominator of each mandrill in the horde. Dominator assignment replicates the mandrill social hierarchy by ranking particles according to fitness values. To imitate this, research builds a parameter named α , which decreases linearly from 1 to 0 as the optimization process progresses. The equation for calculating α is given by Eq. (19).

$$\alpha = 1 - \frac{current\ iteration}{max\ iteratiatin} \tag{19}$$

As a result, as iterations pass, the chance of a child being ventral reduces as given by Eq. (20) and the attendance rate B(t) at iteration t is computed using the following Eq. (21).

$$ventrality = \alpha < random(0,1)$$
 (20)

$$B(t) = M \times |L + (U - L) \times \alpha| \tag{21}$$

The percentage of male participants at iteration t is given by B(t), whereas L and U are the lower and upper bounds. This is mathematically expressed as follows: Eq. (22).

$$P_j = \frac{f_k}{\sum_{k=1}^n f_k} \tag{22}$$

The chance of the j^{th} mandrill winning the competition is represented by P_i , the fitness value of the j^{th} mandrill is represented by f_k , and the number of male mandrills competing is represented by n.

3.8 Finding radius vector

The velocity or ideal distance of a particle is essential for updating its location. In this suggestion, the term radius refers to an ellipsoidal-based method for creating points. Finding the ideal radius vector throughout the space's dimensions is essential to the algorithm's performance, as given by Eq. (23).

$$D_{p_j} = \sqrt{\sum_{k=1}^{d} \left(P_{d_j} - P_{p_j} \right)^2}$$
 (23)

The dimensionality of the solution space is indicated by d, while the U-th dimension of the dominator and the i-th position of the particle are represented by P.

3.9 Ellipsoidal new solution generation

The ellipsoidal new solution generation mechanism is an innovative technique for solution generation inside metaheuristic optimization algorithms. This technique increases the algorithm's durability as the ellipsoid is completely encompassed within the hypercube defined by the same distance vector (radius vector). The ellipsoidal technique removes superfluous areas for fresh solution generation from the hypercube as provided by Eq. (24).

$$(x-c)^T A^{-1}(y-c) \le 1 \tag{24}$$

Where B is a positive-definite shape matrix, c is the center of the ellipsoid, and y is the candidate solution vector. The MCLSM-AE model has a unique benefit in EVCD forecasting by appropriately incorporating both spatial and temporal dependencies by utilizing CNN and LSTM components, respectively. The result is extremely accurate and robust predictions that are beyond existing techniques. Algorithm 1 depicts the Pseudocode for the MCLSM-AE model.

Algorithm1: MCLSM-AE)

```
Input:
```

```
- Objective function F(x)
```

- Number of mandrills (n)

- Dimensions of the search space (d)

- Lower and upper bounds of search space (L, U)

Maximum number of iterations (Max_iter)

Output:

- Best solution found (X_best)

Best fitness value (F_best)

Step 1: Initialize the position matrix P [n

 \times d] using semi greedy strategy:

For i = 1 to n:

Set P[i][0] to segment i of dimension 1

For j = 1 to d - 1:

Set P[i][j] randomly in [L[j], U[j]]

Step 2: Evaluate initial fitness f_k

 $= F(P[k]) \forall k \in \{1, 2, ..., n\}$

Step 3: For t = 1 to Max_iter do:

Step 4: *Update alpha* (α) *using Eq.* (19):

Step 5: Compute attendance rate B(t) using Eq. (21):

Step 6: *Assign dominators*: Sort all mandrills by fitness (ascending)

Assign top B(t) mandrills as dominators

For each mandrill j = 1 to n: Step 7:

Step 8: Evaluate ventrality using Eq. (20)

Step 9: Select a dominator (based on P_j in Eq. 22)

Step 10: Calculate Radius Vector D_pj using Eq. (23):

Step 11: Generate ellipsoidal new solution y using Eq. (24)

Step 12: If y is inside bounds [L, U]:

Evaluate fitness $f_y = F(y)$

If $f_y < f_j$:

Replace $P[j] \leftarrow y$

 $f_j \leftarrow f_y$

Step 13: End For

```
Step 14: Update global best:

If any f_{-j} < F_{-}best:

X_{-}best \leftarrow P[j]

F_{-}best \leftarrow f_{-j}

Step 15: End For

Return X_{-}best, F_{-}best
```

4 Result

The main aim of the study was to create a reliable and close forecasting model for EVCD based on an MCLSM-AE model. This section contains the description of the experimental setup, and prediction metrics used to predict the EVCD.

4.1 Experimental setup

The experimental setup was executed in Python with the TensorFlow and Keras libraries on a PC system with an Intel Core i7 processor, NVIDIA RTX 3080 GPU and 32GB RAM. The models were tested and trained on a 1TB SSD storage with Windows 11 to help manage data efficiently and make it more efficient to perform computations.

4.2 Outcome of performance metrics

The performance metrics used to forecast the EVCD, such as convergence curve, and charging time prediction time.

4.2.1 Convergence curve

The convergence curve shows how the optimization process reduces the loss or error along iterations. It shows the efficiency and strength of the model training process in attaining optimal EVCD forecasting performance, as illustrated in the Figure 4.The convergence curve of the MCLSM-AE model displays a precipitous decline in fitness from the initial level of approximately 1.72×10^6 to the terminal value of approximately 1.24×10^6 in the first 40 iterations, which shows efficient optimization and faster convergence compared to usual methods, and confirms the high-level learning and predictive power of the MCLSM-AE in EVCD forecasting.

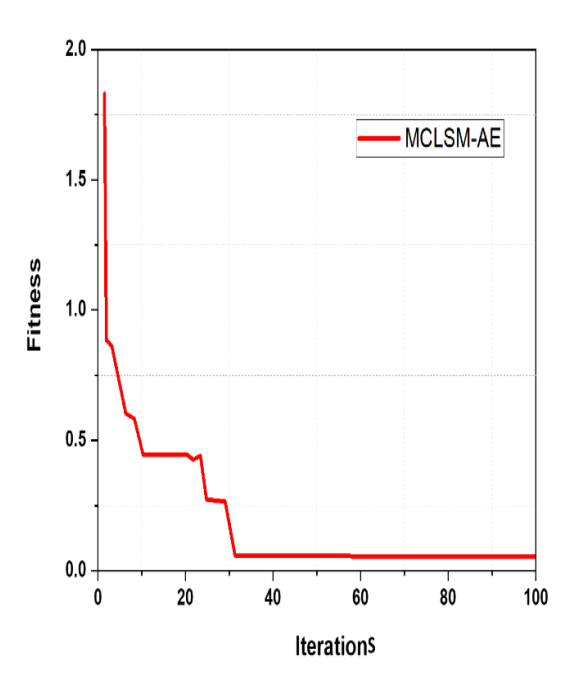


Figure 4: Convergence curve for EVCD Forecasting

4.2.2 Charging demand forecasting time

Charging demand forecasting time refers to the time a forecasting model takes to precisely predict future EVCD using the historical and real-time information. It is essential to facilitate timely energy distribution, grid operation optimization, and removal of charging delays in smart city infrastructures. Visual representation of the charging demand forecasting time was illustrated in Figure 5.

Fig.5 shows the forecasted charging demand over time by using the MCLSM-AE model, which begins at 10 units and increases smoothly to 65 units for a 4-hour period. The curve shows that the model can reproduce the nonlinear trend of increasing growth in CD accurately.

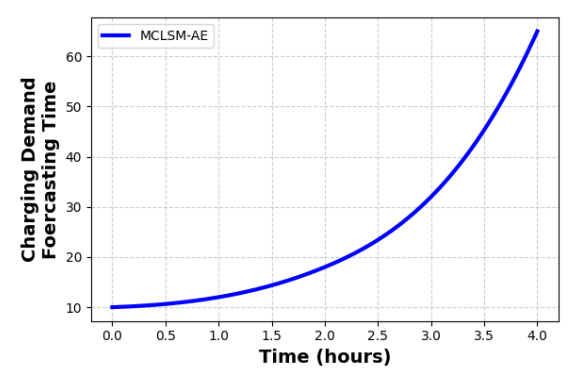


Figure 5: Charging demand forecasting time

4.3 Comparison phase

In this segment, performance indicators like Mean Absolute Error (MAE), RMSE, Mean Absolute Percentage Error (MAPE) and MSE to predict the EVCD using MCLSM-AE model. MCLSM-AE was compared to base models which are already present such as empirical mode decomposition with arithmetic optimization algorithm and deep LSTM combined (EMD-AOA-DLSTM) [22], PAG [23] and Fusion graph convolutional network with enhanced gate recurrent unit and Red Kite Optimization Algorithm (FGCN-EGRU-RKOA) [24], which all were used for prediction of EV charging demand.

4.3.1. Mean absolute error (MAE)

MAE computes the average magnitude of errors between predicted and actual values irrespective of their direction. It was utilized to measure the accuracy of EVCD predictions, which helps in determining how well the MCLSM-AE's predictions compare against actual values.

$$MAE = \frac{1}{n} \sum_{i=1}^{n} |y_i - \hat{y}_i| \tag{1}$$

4.3.2. Root mean square error (RMSE)

RMSE provides a simple evaluation of the amount of the model prediction error by quantifying the square root of the average of squared discrepancies between actual and forecasted values. Lower RMSE illustrates better generalizability and predictability.

$$RMSE = \sqrt{\frac{1}{n} \sum_{i=1}^{n} (y_i - \hat{y}_i)^2}$$
 (2)

4.3.3. Mean Squared Error (MSE)

MSE is a mean of the squared errors between the expected and the real values, giving more importance to important errors. Lower MSE means the model is effectively minimizing prediction error in training and

$$MSE = \frac{1}{n} \sum_{i=1}^{n} (y_i - \hat{y}_i)^2$$
 (3)

4.3.4. Mean absolute percentage error (MAPE)

MAPE analyzes the average total percentage error between the projected and the real data to yield a normalized error measure. It is particularly valuable for assessing forecast precision at various EV charging load demand levels. A lower MAPE value shows that the forecasting model is stronger and relevant to realworld applications.

$$MAPE = \frac{1}{n} \sum_{i=1}^{n} \left| \frac{y_i - \vec{y}_i}{y_i} \right| \tag{4}$$

Figure 6 illustrates the graphical representation of RMSE and MSE using the MCLSM-AE model for EVCD prediction. The EMD-AOA-DLSTM [22] approach reported an RMSE of 0.000020628 and MAE of 0.1083, which shows relatively higher errors than the other approaches. The PAG [23] approach gave much better results with an RMSE of 0.0548 and MAE of 0.0333, displaying improved accuracy. The FGCN-EGRU-RKOA approach gave moderate results with an RMSE of 0.1735 and MAE of 0.3228. Conversely, the MCLSM-AE had excellent performance with RMSE of 0.000004 and MAE of 0.0275, superior to that of all the other models, which also showed its high accuracy and reliability in the forecasting task. Table 3 shows the RMSE and MAE of MCLSM-AE for EVCD prediction.

Table 3: RMSE and MAE values of the MCLSM-AE model for EVCD prediction

Method	RMSE	MAE
S		
EMD-	0.000020628	0.1083
AOA-		
DLSTM		
[22]		
PAG	0.0548	0.0333
[23]		
FGCN-	0.1735	0.3228
EGRU-		
RKOA		
[24]		
MCLS	0.000014832 ± 0.00	0.0275 ± 0.0
M-AE	00012	011
[Propos	00012	VII
ed]		

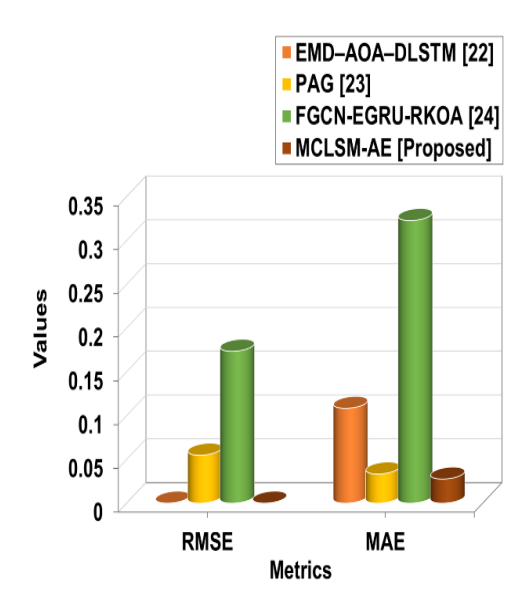


Figure 6: Graphical Representation of RMSE and MAE using MCLSM-AE model for EVCD prediction

Table 4 and Figure 7 show the model evaluation of MSE for MCLSM-AE with the existing method. The MCLSM-AE method demonstrates superior performance with an MSE of 0.0000015, while the other methods, such as EMD-AOA-DLSTM [22] (0.00004255) and FGCN-EGRU-RKOA [24] (0.0301), show comparatively poor results.

Table 4: Model Evaluation Table of MSE for MCLSM-AE with Existing Method

Methods	MSE
EMD-	0.00004255
AOA-	
DLSTM	
[22]	
FGCN-	0.0301
EGRU-	
RKOA	
[24]	
MCLSM-	$0.00000000022 \pm 0.000000000$
AE	05
[Proposed	
l i	

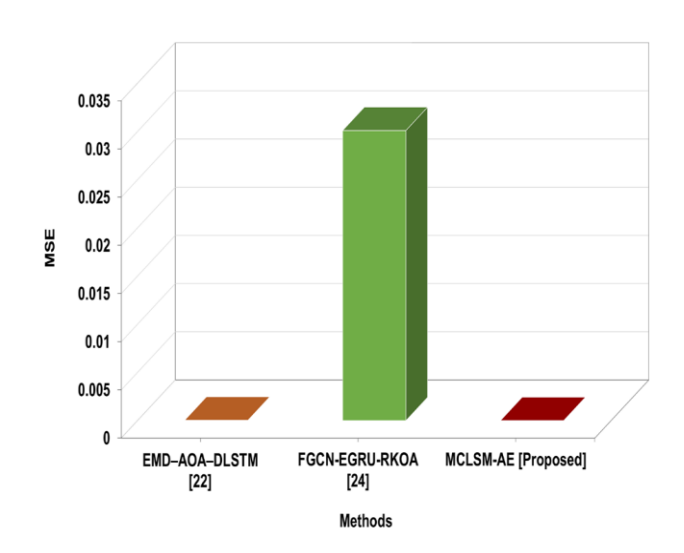


Figure 7: Performance Comparison of MSE across Different Models for EVCD Prediction

Table 5 and Figure 8 illustrate the MAPE-based performance comparison between PAG and MCLSM-AE models. The proposed MCLSM-AE model achieves a lower MAPE of 0.0934, compared to 0.1687 for the PAG [23] method, indicating improved accuracy.

Table 5: Summary of the MAPE value for the MCLSM-AE

Methods	MAPE
PAG [23]	0.1687
MCLSM-AE [Proposed]	0.0934 ±0.0043

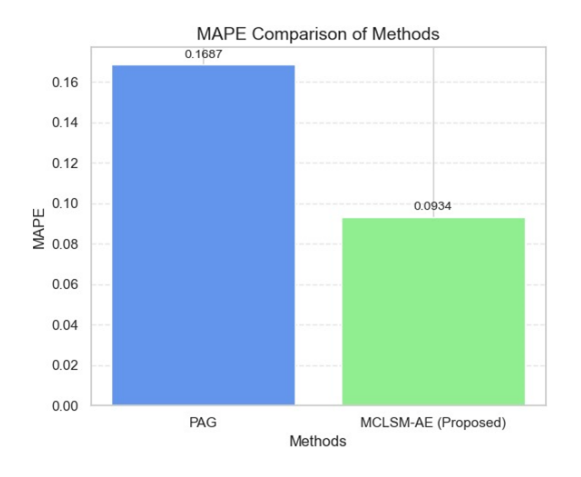


Figure 8: MAPE-Based Performance Comparison between PAG [23] and MCLSM-AE

Figure 9 depicts the 5-fold cross validation and average values facilitating more effective energy distribution and infrastructure planning.

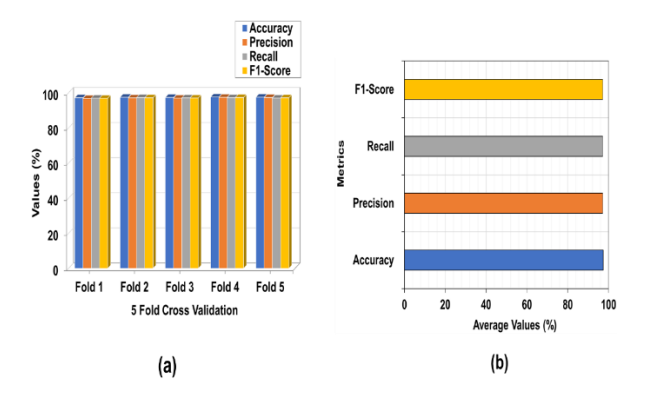


Figure 9: Outcome of (a) 5-Fold Cross Validation (b) average values

4.4 Discussion

The MCLSM-AE approach has a lower MAPE of 0.0934, which shows better accuracy in prediction than the PAG [23] approach with a MAPE of 0.1687. The research proposed an advanced hybrid MCLSM-AE model to predict the EVCD. There are some limitations of existing models like EMD-AOA-DLSTM [22], PAG [23], and FGCN-EGRU-RKOA [24]. EMD-AOA-DLSTM [22] and FGCN-EGRU-RKOA [24] have high RMSE and MAE values, reflecting poor accuracy and ineffective noise and spatial-temporal dependency handling. Model like PAG [23] does not provide holistic error reporting, which degrades the evaluation quality. However, MCLSM-AE achieves a better performance compared to the below models with least RMSE, MAE, and MSE, indicating higher precision. Its strong robustness, noise resistance, and dynamic learning provide a better solution to actual real-world CD of EVs. The MCLSM-AE model greatly improved the EVCD prediction accuracy, facilitating more effective energy distribution and infrastructure planning. This helps in more intelligent grid management and sustainable development of electric mobility.

Conclusion 5

The MCLSM-AE model was successfully developed and validated for estimating EVCD with the introduction of the MOA, AE, CNN-LSTM, and attention mechanism. The model was successfully trained on a dataset comprising historical EV charging data, traffic patterns, weather information, and spatial grid mappings. The model addressed complex spatialtemporal patterns and noisy behaviors by applying methods. rigorous preprocessing including normalization, MVI, and feature reduction. The implementation of MOA allowed for intelligent hyperparameter fine-tuning, while CNN and LSTM captured spatial and temporal trends, respectively. The model outperformed baseline methods, decreasing with a reduced RMSE of 0.000004. However, the research was limited by the availability and quality of real-time charging and traffic metrics, and the model's generalizability across regions was not properly validated. Future research could focus on real-time adaptive learning, integration with Renewable Energy (RE) sources, and deployment in a variety of urban settings to improve the scalability and effectiveness of the EV infrastructure planning and the energy management. Future work focuses on incorporating these tests to rigorously validate the improvements of the proposed model over baseline methods.

References

- [1] Xingjun, H., Mao, Z., Lin, Y., Shi, Q., Liu, F., & Zhou, F. (2024). Sharing or privacy for private electric vehicle charging piles? Evidence from Chongqing. Technological Forecasting and Social 203, Change, https://doi.org/10.1016/j.techfore.2024.123350
- Mei, Z., Que, Z., Qiu, H., Zhu, Z., & Cai, Z. (2023). Optimizing the configuration of electric vehicle charging piles in public parking lots based on a multi-agent model. Physica A: Statistical Mechanics and Its Applications, 632, 129329. https://doi.org/10.1016/j.physa.2023.129329
- [3] Liu, Z., Liang, X., Li, L., Li, X., & Ou, W. (2024). Research on sustainable design of smart charging pile based on machine learning. Symmetry, 16(12), 1582. https://doi.org/10.3390/sym16121582
- [4] Ma, S. C., & Fan, Y. (2020). A deployment model of EV charging piles and its impact on EV promotion. Energy Policy, 146, 111777. https://doi.org/10.1016/j.enpol.2020.111777
- [5] Wu, J., Su, H., Meng, J., & Lin, M. (2023). Electric vehicle charging scheduling considering infrastructure constraints. Energy, 278, 127806. https://doi.org/10.1016/j.energy.2023.127806
- [6] Zheng, Y., Liu, D., An, F., Wang, J., Gao, X., & Jia, N. (2025). Impact of charging infrastructure construction on electric vehicle diffusion based on a multi-agent model. iScience, 28(4). https://doi.org/10.1016/j.isci.2025.112257
- Kang, J., Kong, H., Lin, Z., & Dang, A. (2022). Mapping the dynamics of electric vehicle charging demand within Beijing's spatial structure. Sustainable Cities and Society, 76, 103507.
 - https://doi.org/10.1016/j.scs.2021.103507
- Xing, Q., Chen, Z., Zhang, Z., Xu, X., Zhang, T., Huang, X., & Wang, H. (2020). Urban electric vehicle fast-charging demand forecasting model based on data-driven approach and human decision-making behavior. Energies, 13(6), 1412. https://doi.org/10.3390/en13061412

- [9] Jiang, Q., Zhang, N., He, B. Y., Lee, C., & Ma, J. (2024). Large-scale public charging demand prediction with a scenario-and activity-based approach. *Transportation Research Part A: Policy and Practice*, 179, 103935. https://doi.org/10.1016/j.tra.2023.103935
- [10] Deng, S., Wang, J., Tao, L., Zhang, S., & Sun, H. (2023). EV charging load forecasting model mining algorithm based on hybrid intelligence. *Computers & Electrical Engineering*, 112, 109010. https://doi.org/10.1016/j.compeleceng.2023.109 010
- [11] Liu, X. (2022). Bi-level planning method of urban electric vehicle charging station considering multiple demand scenarios and multi-type charging piles. *Journal of Energy Storage*, 48, 104012. https://doi.org/10.1016/j.est.2022.104012
- [12] Chen, J., Li, F., Yang, R., & Ma, D. (2020). Impacts of increasing private charging piles on electric vehicles' charging profiles: A case study in Hefei City, China. *Energies*, *13*(17), 4387. https://doi.org/10.3390/en13174387
- [13] Li, J., Zou, W., Yang, Q., Yao, F., & Zhu, J. (2024). EV charging fairness protective management against charging demand uncertainty for a new "1 to N" automatic charging pile. *Energy*, 306, 132428. https://doi.org/10.1016/j.energy.2024.132428
- [14] Zhang, Y., Wang, Y., Li, F., Wu, B., Chiang, Y. Y., & Zhang, X. (2020). Efficient deployment of electric vehicle charging infrastructure: Simultaneous optimization of charging station placement and charging pile assignment. *IEEE Transactions on Intelligent Transportation Systems*, 22(10), 6654–6659. https://doi.org/10.1109/TITS.2020.2990694
- [15] Li, Z., Wu, X., Zhang, S., Min, L., Feng, Y., Hang, Z., & Shi, L. (2023). Energy storage charging pile management based on Internet of Things technology for electric vehicles. *Processes*, 11(5), 1561. https://doi.org/10.1155/2022/8533219
- [16] Yi, T., Zhang, C., Lin, T., & Liu, J. (2020). Research on the spatial-temporal distribution of electric vehicle charging load demand: A case study in China. *Journal of Cleaner Production*, 242, 118457. https://doi.org/10.1016/j.jclepro.2019.118457
- [17] Li, H., Qu, H., Tan, X., You, L., Zhu, R., & Fan, W. (2025). UrbanEV: An open benchmark dataset for urban electric vehicle charging demand prediction. *Scientific Data*, 12(1), 523. https://doi.org/10.1038/s41597-025-04874-4
- [18] Kuang, H., Deng, K., You, L., & Li, J. (2025). Citywide electric vehicle charging demand prediction approach considering urban region and dynamic influences. *Energy*, 320, 135170. https://doi.org/10.1016/j.energy.2025.135170

- [19] Pourvaziri, H., Sarhadi, H., Azad, N., Afshari, H., & Taghavi, M. (2024). Planning of electric vehicle charging stations: An integrated deep learning and queueing theory approach. Transportation Research Part E: Logistics and Transportation Review, 186, 103568. https://doi.org/10.1016/j.tre.2024.103568
- [20] Wang, S., Zhuge, C., Shao, C., Wang, P., Yang, X., & Wang, S. (2023). Short-term electric vehicle charging demand prediction: A deep learning approach. *Applied Energy*, 340, 121032. https://doi.org/10.1016/j.apenergy.2023.121032
- [21] Koohfar, S., Woldemariam, W., & Kumar, A. (2023). Prediction of electric vehicles charging demand: A transformer-based deep learning approach. *Sustainability*, 15(3), 2105. https://doi.org/10.3390/su15032105
- [22] Shanmuganathan, J., Victoire, A. A., Balraj, G., & Victoire, A. (2022). Deep learning LSTM recurrent neural network model for prediction of electric vehicle charging demand. *Sustainability*, *14*(16), 10207. https://doi.org/10.3390/su141610207
- [23] Qu, H., Kuang, H., Wang, Q., Li, J., & You, L. (2024). A physics-informed and attention-based graph learning approach for regional electric vehicle charging demand prediction. *IEEE Transactions on Intelligent Transportation Systems*. https://doi.org/10.1109/TITS.2024.3401850
- [24] Gunasekaran, R., Pareek, P. K., Gupta, S., & Shukla, A. (2024). Prediction of electric vehicle charging demand using enhanced gated recurrent units with RKOA based graph convolutional network. *Discover Applied Sciences*, *6*(11), 1–18. https://doi.org/10.1007/s42452-024-06326-x